

## Accepted Manuscript

Surface Flow Measurements From Drones

Flavia Tauro, Maurizio Porfiri, Salvatore Grimaldi

PII: S0022-1694(16)30363-8

DOI: <http://dx.doi.org/10.1016/j.jhydrol.2016.06.012>

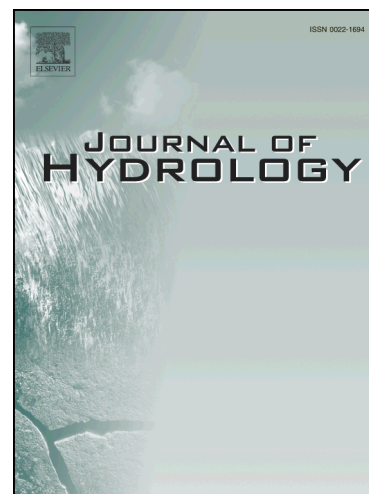
Reference: HYDROL 21330

To appear in: *Journal of Hydrology*

Received Date: 10 January 2016

Revised Date: 13 April 2016

Accepted Date: 4 June 2016



Please cite this article as: Tauro, F., Porfiri, M., Grimaldi, S., Surface Flow Measurements From Drones, *Journal of Hydrology* (2016), doi: <http://dx.doi.org/10.1016/j.jhydrol.2016.06.012>

This is a PDF file of an unedited manuscript that has been accepted for publication. As a service to our customers we are providing this early version of the manuscript. The manuscript will undergo copyediting, typesetting, and review of the resulting proof before it is published in its final form. Please note that during the production process errors may be discovered which could affect the content, and all legal disclaimers that apply to the journal pertain.

# Surface Flow Measurements From Drones

Flavia Tauro<sup>a</sup>, Maurizio Porfiri<sup>b</sup>, Salvatore Grimaldi<sup>a,b,1,\*</sup>

<sup>a</sup>*Dipartimento per l'Innovazione nei sistemi Biologici, Agroalimentari e Forestali,  
University of Tuscia, Viterbo, Italy.*

<sup>b</sup>*Department of Mechanical and Aerospace Engineering, New York University Tandon  
School of Engineering, Brooklyn, NY 11201, USA.*

---

## Abstract

1 Drones are transforming the way we sense and interact with the environment.  
2 However, despite their increased capabilities, the use of drones in geophysical  
3 sciences usually focuses on image acquisition for generating high-resolution  
4 maps. Motivated by the increasing demand for innovative and high perfor-  
5 mance geophysical observational methodologies, we posit the integration of  
6 drone technology and optical sensing toward a quantitative characterization  
7 of surface flow phenomena. We demonstrate that a recreational drone can be  
8 used to yield accurate surface flow maps of sub-meter water bodies. Specifi-  
9 cally, drone's vibrations do not hinder surface flow observations, and velocity  
10 measurements are in agreement with traditional techniques. This first in-  
11 stance of quantitative water flow sensing from a flying drone paves the way  
12 to novel observations of the environment.

*Keywords:* Flow measurement, Surface Hydrology, Large Scale Particle  
Image Velocimetry, Unmanned Aerial Vehicle

---

\*Corresponding author

*Email address:* [salvatore.grimaldi@unitus.it](mailto:salvatore.grimaldi@unitus.it) (Salvatore Grimaldi)

<sup>1</sup>Ph.: +39 0761 357326; Fax: +39 0761 357356

## 13 1. Introduction

14 Surface waters influence the way the landscape evolves, ecosystems de-  
15 velop, environmental risks arise, and epidemics propagate [1, 2, 3, 4]. Due  
16 to the complexity of surface water processes, a unique observational method  
17 for identifying and quantitatively monitoring flows is yet to be found [5].  
18 Traditionally, surface flows are invasively monitored using current meters [6],  
19 tracing systems [7], and acoustic doppler instrumentation [8]. Water control  
20 structures, such as weirs and spillways, can also be used to estimate flow  
21 discharge [9].

22 Even if the efficacy of such methods has been demonstrated in the tech-  
23 nical literature [10], their use is limited to easy-to-access environments. In  
24 addition, the measurement accuracy can be affected by the severity of natural  
25 rainfall events and by systematic errors associated with sensors interfering  
26 with the flow. To address some of these challenges, considerable efforts have  
27 been devoted toward the development and refinement of remote methods,  
28 including hand-held radars [11], microwave sensors [12], and satellites [13].  
29 These approaches have highly benefitted the realm of hydrological observa-  
30 tions; however, most of them are only applicable to large scale channel flows,  
31 may be expensive, and may not be suitable to frequently monitor water bod-  
32 ies.

33 To mitigate such issues, several methods based on the remote acquisition  
34 and analysis of flow images have been proposed and implemented in the last  
35 two decades [14]. Specifically, in [15], images of large scale riverine ecosys-  
36 tems are analyzed through high-speed cross-correlation to obtain surface flow  
37 velocity maps. These surface flow velocity maps can be complemented with

38 information on the bathymetry to allow for flow discharge estimations [16].  
39 Such optical observational methods are challenged by practical difficulties,  
40 such as the need for collecting ground reference points [17], and, therefore,  
41 flow data are often not available at ungauged sites, such as extra-urban areas,  
42 large-scale lakes and glaciers, coasts, and river estuaries. Despite practical  
43 limitations, optical methods are inherently suited to enable continuous and  
44 remote observations over diverse water bodies, spanning from rills to large  
45 scale rivers. Notably, the potential of such image-based methods has been  
46 assessed on a mountainous stream [18], a semi-natural hillslope [19], and a  
47 large scale river [17].

48 Here, we propose a novel, fully remote approach for surface flow obser-  
49 vations that overcomes practical difficulties related to the implementation  
50 of optical methods in difficult-to-access environments. Specifically, we put  
51 forward the integration of optical observational techniques and drones for  
52 non-invasive quantitative flow measurement. With more than six billion  
53 dollars a year spent in research and development around the world [20],  
54 drones have transformed our capacity to remotely sense and access the en-  
55 vironment [21, 22, 23, 24]. For instance, in the last decade, drones have  
56 empowered multiple fields of science by enabling data collection in hostile  
57 environments, such as volcanoes [25] and ice sheets [26], and by providing  
58 footage over extended areas, such as forests [22] and natural reserves [27].  
59 Just as aerial and satellite sensing have transformed scientific observations,  
60 allowing the resolution of large-scale physical processes [28, 29], the pervasive  
61 use of drones is set to revolutionise geophysical sciences through the rapid  
62 and refined measurement of small to medium scale phenomena.

63 In the realm of hydrology, drones have the potential to enable remote and  
64 distributed flow measurements in difficult-to-access water environments dur-  
65 ing adverse hydro-meteorological events. In our vision, a drone is deployed  
66 in natural environments and is remotely piloted (or, alternatively, guided  
67 through GPS waypoint trajectory) above the water body of interest upon  
68 request/need of the operator. An onboard camera oriented with its axis per-  
69 pendicular to the water surface captures videos of the water surface, whereby  
70 a ground user identifies a region of interest through a wireless monitor in real  
71 time. Once the ground user selects an area of interest, the drone is set to the  
72 hovering mode, and the platform stationkeeps above the region while taking  
73 high-resolution videos of the water surface. Pictures extracted from the drone  
74 footage can be processed off-line through several optical-based algorithms to  
75 extract the surface velocity field.

76 To demonstrate the potential of our approach, here, we present the design  
77 and preliminary assessment of a novel aerial sensing platform. The platform  
78 features a low-cost recreational drone equipped with a miniature camera and  
79 a system of lasers to remotely assign metric dimensions to images (remote  
80 photometric calibration in the rest of the note) without the acquisition of  
81 ground reference points. To assess the feasibility of the hovering capability  
82 of the drone for reliable flow velocimetry, we execute preliminary experiments  
83 on an ad hoc developed outdoor controlled facility at University of Tuscia.  
84 Finally, we perform surface flow observations in a small scale stream (less  
85 than 1 m wide and a few centimeters deep) in the Italian Alps. Interestingly,  
86 few noninvasive techniques are currently available to monitor small scale sur-  
87 face flows in natural environments. We remotely capture and calibrate videos

88 of the stream from the drone and apply the Large Scale Particle Image Ve-  
89 locimetry (LSPIV) high-speed cross-correlation algorithm [16] that extracts  
90 usable flow velocity maps from the motion of stream floaters. Such drone-  
91 based surface flow velocity estimates are compared to benchmark values from  
92 a current meter to demonstrate the validity of airborne flow velocimetry.

93 Our method is expected to help in hydrological monitoring in ungauged  
94 areas by providing information on the kinematics of surface waters. Differ-  
95 ently from standard drone-based monitoring where image mosaicing tech-  
96 niques are used to assemble maps [30], our approach treats captured videos  
97 as quantitative data and analyzes them to measure the surface flow velocity.  
98 These observations could leverage current knowledge on the contribution of  
99 surface flows to the overall hydrological response of natural systems. Further,  
100 continuous technological advancements in battery life and camera storage ca-  
101 pacity may foster observations at the catchment scale and in large scale and  
102 yet ungauged water systems, thus opening novel research avenues in hydrol-  
103 ogy.

104 The rest of the technical note is organized as follows. In Section 2, the  
105 aerial sensing platform, experimental settings, and image-based procedures  
106 are presented. In Section 3, we report experimental findings for the hovering  
107 assessment and the airborne flow velocimetry. In Section 4, we discuss the  
108 advancements of the proposed approach. Section 5 is left for conclusions.

## 109 2. Materials and Methods

110 Here, we present the aerial sensing platform utilized in the experiments.  
111 Further, we provide details for the hovering assessment and the airborne flow

112 velocimetry experiments.

### 113 *2.1. Aerial Sensing Platform*

114 The aerial sensing platform features a DJI Phantom 2 quadrotor [31]  
115 mounting a Zenmuse H3-2D gimbal and a GoPro Hero 3 camera oriented  
116 with its axis along the perpendicular. This configuration allows for compen-  
117 sating the drone vibrations about the pitch and roll axes, while minimizing  
118 distortions in video capture due to the inclination of the camera axis with  
119 respect to the field of view (FOV). Remote photometric calibration is en-  
120 abled through four green lasers (532 nm in wavelength and less than 5 mW  
121 in power) installed at the four corners of the fuselage along the drone's yaw  
122 axis. The platform is less than 1.5 kg in weight and its overall cost is €1,300.

123 The relative distances of the laser pointers are measured upon assembly  
124 of the sensing platform with a precision caliper. This system of lasers has  
125 the twofold objective of: i) focusing points at known distances in the FOV  
126 for remote image calibration and ii) indicating possible elevation and atti-  
127 tude changes during hovering from the relative distance of the laser traces  
128 in the images [17]. With respect to i), the traces of the lasers in captured  
129 videos are used to estimate pixel dimensions in metric units. With respect to  
130 ii), inaccurate hovering leads to images that depict slightly different FOVs.  
131 However, high-speed cross-correlation should be applied on images display-  
132 ing consistent regions of the fluid domain [32]. To this aim, lasers can be  
133 instrumental to automatically identify portions of footage captured while the  
134 drone is hovering at a given location. In fact, the traces that lasers determine  
135 on the ground vary, based on the elevation and attitude of the drone; there-  
136 fore, sequences of images displaying similar traces can be directly processed

137 for surface flow velocity estimation.

## 138 *2.2. Hovering Assessment*

139 A preliminary experiment assessment is conducted to assess the feasibility  
140 of using a commercial low-cost platform for airborne flow velocimetry. The  
141 aerial sensing platform presents limited hovering capability (vertical:  $\pm 0.8$  m  
142 and horizontal:  $\pm 2.5$  m [31]). Therefore, airframe changes in attitude and  
143 elevation may lead to variable image FOVs [33, 34]. To evaluate such FOV  
144 variations, we fly the platform in the hovering mode above a large scale grid  
145 in an outdoor facility at the University of Tuscia, Italy. We perform a 22 s  
146 flight, whereby the onboard GoPro frame rate is set to 60 Hz and the FOV  
147 to medium (focal length equal to 21 mm). The experiment is conducted at  
148 dusk and during light air wind conditions (2.19 km/h wind speed) [35].

149 Hovering capability is assessed by estimating the relative variations in the  
150 pixel area of the grid cells captured by the drone during the flight. Slight  
151 variations in the pixel areas of the grid cells during the flight would suggest  
152 that changes in the drone's elevation and attitude can be mitigated with  
153 minimal image processing, and, therefore, drone-based videos are compatible  
154 with accurate surface flow observations. To provide a reliable assessment, the  
155 experimental time is set to 22 s, whereas airborne flow velocimetry tests only  
156 last up to few seconds ( given the high camera frame rate, video data recorded  
157 in few seconds are largely sufficient for accurate measurements).

### 158 *2.2.1. Hovering Assessment Outdoor Facility*

159 The drone is flown above a  $5 \times 5$  m<sup>2</sup> flat grid assembled in the outdoor  
160 laboratory at University of Tuscia, Italy, out of a dark opaque ground cloth



161 and a structure of white strings. The strings are laid to create  $1 \times 1 \text{ m}^2$   
162 squared grid cells. The dark cloth minimizes reflections and enhances the  
163 visibility of the white strings against the background. Figure 1 presents a  
164 schematics of the setup. The drone is deployed to hover above the center of  
165 the grid. The dashed red rectangle in Figure 1 shows the FOV captured by  
166 the onboard camera. The laser-focused rectangle is indicated in yellow.

### 167 *2.2.2. Image-based Hovering Evaluation*

168 Captured video data are preliminary corrected for the camera lens dis-  
169 tortion. The video fish eye distortion is removed through the freely available  
170 GoPro Studio 2.0 Software. Then, the video is converted and decompressed  
171 to extract Full HD frames. Image processing entails a preliminary phase in  
172 which frames are converted to grayscale based on luminance information and  
173 then converted to binary by imposing a threshold. Image segmentation is  
174 then applied on binary images to retain essential features.

175 To estimate the pixel area of the grid cells, an artificial binary template  
176 depicting a representative node of the grid is created. Normalized cross-  
177 correlation is performed between the template and images extracted from  
178 the experimental video. By retaining locations presenting high values of the  
179 cross-correlation coefficient and repairing false correlations, the pixel loca-  
180 tions of the grid nodes are obtained. Image-based algorithms [36, 37] are  
181 utilized to compute the areas of the grid cells and the area of the rectangle  
182 identified by the four lasers.

183 *2.3. Airborne Flow Velocimetry*

184 To ultimately demonstrate the potential of drone-based flow observa-  
185 tions, surface flow measurements are conducted over a less than 1 m-wide  
186 and 11 cm-deep mountainous stream in the Rio Cordon natural catchment,  
187 Italy [18].

188 *2.3.1. Airborne Flow Velocimetry Study Site*

189 The Rio Cordon drains a 7.68 km<sup>2</sup> natural basin located in the Dolomites,  
190 Northeastern Italy. The stream is a tributary of the Fiorentina stream that in  
191 turn flows into the Rio Cordevole. The catchment drainage network extends  
192 for approximately 19 km at an average slope of 47.85%. Tests are executed  
193 at a local gauging station, which is equipped with water gauges, a coarse  
194 sediment grille, and a diversion pool for water and finer material. The gaug-  
195 ing station is located at 1763 m above sea level where the area drained by  
196 the stream is approximately 5 km<sup>2</sup> large. At the time of the experiments, a  
197 nearby meteorological station recorded a wind speed of 0.9 m/s.

198 *2.3.2. Airborne Flow Velocimetry Procedure*

199 The drone is flown above an artificially channeled stream reach located  
200 in the proximity of a stream gauge. The selected stream reach is a rectilinear  
201 tract with a concrete rectangular section that extends for approximately  
202 10 m. Surface velocity is measured using both artificial and natural tracers.  
203 Ten repetitions are performed for each type of tracer. Similar to [38, 39],  
204 artificial tracers are high-visibility in-house fabricated particles synthesized  
205 from biocompatible and buoyant children-friendly dough. Particle size ranges  
206 from 0.5 up to 1 cm, and beads are red, yellow, orange, and green in color.

207 Also, experiments are conducted using natural leaves as tracers. In both  
208 classes of experiments, the drone captures Full HD videos at 60Hz frame  
209 rate. On average, the FOV extends for  $9 \times 5 \text{ m}^2$ .

210 Drone-based data are compared to benchmark flow velocities obtained  
211 using an OTT C2 small current meter. Current meters yield accurate and  
212 repeatable open channel flow measurements up to a few centimeters from  
213 the water surface and, differently from more costly non-contact radars, are  
214 widely used by researchers and practitioners in environmental monitoring.  
215 In the experiments, the instrument is set to the time measurement mode,  
216 whereby the number of impulses recorded in 10s are counted and related to  
217 flow velocity. The velocity is measured at a cross-section of the stream a  
218 few centimeters upstream the subarea used for comparing the drone tests.  
219 Benchmark values are obtained by measuring the flow at 0.5m from the  
220 right stream bank (that is, in the center of the stream) and 3 cm underneath  
221 the water surface and averaging over three repetitions. Obtained values are  
222 relative to the uppermost layer of the stream (top 30% of the stream depth),  
223 where the velocity is less influenced by wind effects and, therefore, it is likely  
224 higher than surface velocity.

### 225 *2.3.3. Airborne Flow Velocimetry Video Processing*

226 Similar to Section 2.2.2, drone-based videos are fish-eye undistorted and  
227 sequences of Full HD images are extracted. Similar to the image-based hover-  
228 ing evaluation, lasers' traces onto the stream surface are utilized to manually  
229 identify stable image sequences within videos captured from the drone. The  
230 lasers afford remote photometric calibration of experimental images. Specifi-  
231 cally, the pixel distance between lasers traces is manually estimated in several

232 frames and validated with respect to objects of known dimensions that are  
233 visible in the field of view.

234 Untrimmed images depicting the transit of the tracers are processed using  
235 the high-speed cross-correlation edPIV software [40], where frame acquisition  
236 rate is set to 60 Hz, interrogation window size to  $32 \times 32$  pixels, and grid size  
237 to  $16 \times 16$  pixels. On average, the pixel area displaying the surveyed stream  
238 reach corresponds to 20% of the picture. Surface flow velocity maps are  
239 developed by averaging velocity estimations in time over the sequence of  
240 images analyzed in the experiment.

241 Due to imperfect hovering of the drone during image acquisition, image  
242 portions lying outside the stream presented non-null velocities. To remove  
243 such false readings, the average velocity of nodes outside the stream is au-  
244 tomatically computed and subtracted from the entire set of velocity values.  
245 Given the stability of the aerial platform and the short duration of experi-  
246 mental flights, airframe vibrations do not excessively impact velocity estima-  
247 tion. In particular, velocities estimated without subtracting values of nodes  
248 outside the flow are 5 – 8% larger than measurements herein reported. Com-  
249 parison between measurements executed with the two classes of tracers is  
250 performed by considering a subarea of the stream that is consistently cap-  
251 tured in each video. Then, time-averaged velocities are computed over the  
252 frame sequence and the maximum value of the velocity field in the subarea  
253 is used for comparison.

### 254 3. Results

#### 255 3.1. Hovering Assessment

256 Analysis of images recorded during the hovering test demonstrates that  
257 the platform stability is compatible with airborne flow velocimetry. During  
258 the flight time, consistent portions of the grid are captured by the camera.  
259 Specifically, the 11 grid cells enclosing colored markers in the left panel of  
260 Figure 2 are always visible in frames during the flight. Colored markers inside  
261 such grid cells indicate the average pixel area of each cell over the flight time.  
262 Squares 2, 5, 6, 9, and 10 present smaller areas than squares on the left hand  
263 side of the grid, suggesting that the drone is closer to the left portion of the  
264 grid.

265 In Figure 2 (right), the time series of the areas of the grid cells (colored  
266 dots) and of the laser focused rectangle (black dots) are shown. Due to  
267 illumination conditions, the trace of the four laser beams on the grid is not  
268 always visible (76% of the total number of frames depicted four laser traces).  
269 Notably, the cell areas slightly vary in time, with a maximum coefficient  
270 of variation of 0.89%. On the other hand, external vibrations lead to a  
271 coefficient of variation as large as 2.94% in the time series of the area identified  
272 by the lasers. This is due to the fact that lasers are directly installed on the  
273 drone fuselage, whereas the camera gimbal efficiently mitigates the drone's  
274 vibrations, thus abating the coefficient of variation to less than a third of its  
275 value. We remark that improved stability is crucial for correlation-based flow  
276 velocity estimation, where the similarities between consecutive images are  
277 used to infer the displacement of depicted objects. Therefore, slight changes  
278 in the image FOV due to the drone's vibrations while hovering suggest that

279 reliable cross-correlation is feasible.

### 280 3.2. Airborne Flow Velocimetry

281 Proof of concept velocity observations in the Rio Cordon show the po-  
282 tential of the drone-based approach for surface flow measurement. Aerial  
283 platform velocities measured in the subarea located in between the dark cross-  
284 sectional stripe and the dark inclined stripes (approximately  $0.76 \times 0.83 \text{ m}^2$ ),  
285 Figure 3 (left), are in line with benchmark values, Table 1. Underestimations  
286 with respect to the impeller flowmeter readings may be due to the fact that  
287 the flowmeter is slightly below the water surface (3 cm out of the total depth  
288 of 11 cm), where wind effects are negligible and velocities are expected to be  
289 larger than surface flows.

290 With regards to the two sets of drone measurements in Table 1, differences  
291 between them are not statistically different as determined through one-way  
292 ANOVA ( $F = 2.43$  and  $p = 0.14$ ). The slightly higher uncertainty obtained  
293 in case of natural floaters is attributed to the fact that they were heavily de-  
294 ployed in the stream and, therefore, involved longer flights. Therefore, since  
295 the hovering performance of the drone is reduced over longer flight times, the  
296 use of natural tracers yields the higher standard deviation in Table 1.

297 As shown in the velocity map in Figure 3 (left), the aerial platform is suc-  
298 cessful in monitoring extended portions of the stream and the flow physics  
299 across the stream is accurately captured, Figure 3 (right). Maps from the  
300 drone are slightly affected by local water reflections and areas of poor illumi-  
301 nation, since the onboard camera offers extended FOVs with diffused, rather  
302 than direct, illumination.

#### 303 4. Discussion and Remarks

304 Here, we propose a novel surface flow observation concept based on a  
305 stand-alone sensing platform that integrates drone technology and optical  
306 methods. Not only are image data captured from the platform, but a sys-  
307 tem of lasers enables remote photometric calibration, thus circumventing the  
308 need for time-consuming and expensive field campaigns for GRPs acquisi-  
309 tion. Specifically, in this study, a laser system is utilized for pixel calibration  
310 and for flow velocimetry analyses. Indeed, the stationarity of the time se-  
311 ries of the area identified by the lasers is used to isolate stable sequences for  
312 flow measurements, whereby small variations are associated with instances  
313 of stable hovering.

314 Notably, the laser apparatus paves the way for unsupervised rapid obser-  
315 vations in large scale hydrological systems. Indeed, instances of airborne flow  
316 velocimetry currently rely on the acquisition of fixed objects in the FOV for  
317 photometric calibration and for video stabilization due to imperfect hover-  
318 ing [41, 42, 43]. On the other hand, the use of the laser system will leverage  
319 pixel calibration in the absence of fixed reference objects, thus enabling low  
320 cost observations in large scale systems, such as estuaries and limnological  
321 environments. In such large scale settings that may exceed the maximum dis-  
322 tance range allowed by the remote control, a priori planned GPS waypoint  
323 navigation may facilitate observations.

324 Beyond pixel calibration and video stabilization, analysis of the laser's  
325 traces in the FOV can be used to complement onboard built-in altimetry  
326 measurements. For instance, a smaller area corresponds to a higher distance  
327 of the drone from the ground and, thus, to the drone increasing its vertical

328 position. Therefore, changes in the area and shape of the laser's traces on  
329 the ground can help in estimating the altitude of the drone with respect to  
330 the ground, thus opening the way for refined photometric calibration and  
331 enhanced measurement accuracy.

332 The presented system is inherently suited for real-time analysis in un-  
333 gauged environments. Data acquisition is feasible in rather limited intervals  
334 of time (few seconds) and surface flow velocity map generation is an unsu-  
335 pervised process that can be afforded in 5-10 minutes. In addition, given  
336 the limited cost of the equipment and its ease of implementation (medium  
337 flight skills can be achieved after some hours of training), the approach is  
338 versatile and likely sustainable for most research groups. With regards to  
339 the use of tracers, even if highly-visible artificial tracers enable rapid velocity  
340 estimations, their use requires either the presence of operators or installation  
341 of remotely-operated devices to deploy the particles [18].

342 The dependence of LSPIV measurements on the presence of homoge-  
343 neously distributed tracers may pose a significant technical challenge to prac-  
344 tical implementations of the proposed approach. To overcome this issue, we  
345 envision the development of machine learning techniques to automatically  
346 de-noise pictures [44] and to emphasize floaters' contrast against the image  
347 background. Alternative image-based flow velocimetry algorithms that yield  
348 the trajectory of individual floaters, such as particle tracking velocimetry,  
349 should be explored [45]. In the case of floods or severe events, naturally-  
350 occurring debris and sediments may be sufficient to obtain surface flow ve-  
351 locity measurements [46].

352 The proposed approach may be readily implemented to provide fully



353 remote and rapid flow discharge estimates in inaccessible areas and large  
354 scale ecosystems. For instance, in [47, 48, 49], an entropy-based method  
355 is proposed to estimate flow discharge based on the maximum velocity ob-  
356 served on the stream surface. This approach establishes a linear relation-  
357 ship between the maximum surface velocity and mean velocity in natural  
358 rivers [50, 51]. The integration of such entropy-based approach and drone-  
359 enabled distributed surface velocity observations may lead to flow discharge  
360 estimates in complex environments. Further, application of image mosaicking  
361 and FOV reconstruction techniques may enable surface flow velocity gauging  
362 over large water areas.

## 363 5. Conclusions

364 In this work, we demonstrated the potential of integrating an aerial plat-  
365 form and optical sensing for surface flow measurements in natural environ-  
366 ments. We designed the aerial platform to enable completely remote mea-  
367 surements, thus circumventing the need for on site surveys that are typically  
368 required by traditional measurement techniques, and enabling novel obser-  
369 vations in inaccessible areas. By investigating the hovering capability of the  
370 aerial platform during a flight of more than 20 s, we found that the approach  
371 is suitable for remote flow observations. Further, surface flow velocity mea-  
372 surements performed from the drone on a small scale mountainous stream  
373 were in good agreement with data from on site flow sensing systems.

374 We expect drones to be a forward-looking addition to the experimental  
375 toolbox currently available to hydrologists and geophysicists. As technol-  
376 ogy progresses toward better performing drones, current limitations, such

377 as imperfect hovering capabilities, constrained flight time and payload, will  
378 be easily overcome, and this approach should enable new avenues in hydro-  
379 logical observations. Future studies will be devoted to the application of  
380 the presented methodology to the kinematic characterization of alternative  
381 environmental settings, such as channel and rill flows.

### 382 **Acknowledgements**

383 This work was supported by the Ministero degli Affari Esteri project 2015  
384 Italy-USA PGR00175, by the American Geophysical Union Horton (Hydrology)  
385 Research Grant for Ph.D. students, by the UNESCO Chair in “Water  
386 Resources Management and Culture”, and by the National Science Founda-  
387 tion under grant numbers BCS-1124795 and CMMI-1129820.

- 388 [1] G. E. Tucker, R. L. Bras, Hillslope processes, drainage density, and  
389 landscape morphology, *Water Resources Research* 34 (10) (1998) 2751–  
390 2764.
- 391 [2] A. J. Boulton, S. Findlay, P. Marmonier, E. H. Stanley, H. M. Valett,  
392 The functional significance of the hyporheic zone in streams and rivers,  
393 *Annual Review of Ecology and Systematics* 29 (1998) 59–81.
- 394 [3] V. T. Chow, D. R. Maidment, L. W. Mays, *Applied Hydrology*, McGraw-  
395 Hill, 1988.
- 396 [4] L. Mari, E. Bertuzzo, L. Righetto, R. Casagrandi, M. Gatto,  
397 I. Rodriguez-Iturbe, A. Rinaldo, Modelling cholera epidemics: the role of  
398 waterway, human mobility and sanitation, *Journal of the Royal Society*  
399 *Interface* 9 (103) (2012) 376–388.

- 400 [5] M. Hrachowitz, H. H. G. Savenije, G. Blöschl, J. J. McDonnell, M. Siva-  
401 palan, J. W. Pomeroy, B. Arheimer, T. Blume, M. P. Clark, U. Ehret,  
402 F. Fenicia, J. E. Freer, A. Gelfan, H. V. Gupta, D. A. Hughes, R. W.  
403 Hut, A. Montanari, S. Pande, D. Tetzlaff, P. A. Troch, S. Uhlenbrook,  
404 T. Wagener, H. C. Winsemius, R. A. Woods, E. Zehe, C. Cudennec, A  
405 decade of predictions in ungauged basins (PUB) a review, *Hydrological  
406 Sciences Journal* 58 (6) (2013) 1198–1255.
- 407 [6] A. Tazioli, Experimental methods for river discharge measurements:  
408 comparison among tracers and current meter, *Hydrological Sciences  
409 Journal* 56 (7) (2011) 1314–1324.
- 410 [7] O. Planchon, N. Silvera, R. Gimenez, D. Favis-Mortlock, J. Wainwright,  
411 Y. Le Bissonnais, G. Govers, An automated salt-tracing gauge for flow-  
412 velocity measurement, *Earth Surface Processes and Landforms* 30 (7)  
413 (2005) 833–844.
- 414 [8] T. H. Yorke, K. A. Oberg, Measuring river velocity and discharge  
415 with acoustic Doppler profilers, *Flow Measurement and Instrumenta-  
416 tion* 13 (5–6) (2002) 191–195.
- 417 [9] H. Chanson, *Hydraulics of Open Channel Flow*, Elsevier Butterworth-  
418 Heinemann, Oxford, UK, 2004.
- 419 [10] C. Leibundgut, P. Maloszewski, C. Külls, *Tracers in Hydrology*, Wiley-  
420 Blackwell, Oxford, 2009.
- 421 [11] J. Fulton, J. Ostrowski, Measuring real-time streamflow using emerg-

- 422 ing technologies: radar, hydroacoustics, and the probability concept,  
423 Journal of Hydrology 357 (1–2) (2008) 1–10.
- 424 [12] W. J. Plant, W. C. Keller, K. Hayes, Measurement of river surface cur-  
425 rents with coherent microwave systems, Geoscience and Remote Sensing,  
426 IEEE Transactions on 43 (6) (2005) 1242–1257.
- 427 [13] A. Tarpanelli, S. Barbetta, L. Brocca, T. Moramarco, River discharge  
428 estimation by using altimetry data and simplified flood routing model-  
429 ing, Remote Sensing 5 (9) (2013) 4145–4162.
- 430 [14] I. Fujita, M. Muste, A. Kruger, Large-scale particle image velocime-  
431 try for flow analysis in hydraulic engineering applications, Journal of  
432 Hydraulic Research 36 (3) (1997) 397–414.
- 433 [15] M. Muste, I. Fujita, A. Hauet, Large-scale particle image velocimetry  
434 for measurements in riverine environments, Water Resources Research  
435 44 (4) (2008) W00D19.
- 436 [16] A. Hauet, A. Kruger, W. Krajewski, A. Bradley, M. Muste, J. Creutin,  
437 M. Wilson, Experimental system for real-time discharge estimation using  
438 an image-based method, Journal of Hydrologic Engineering 13 (2) (2008)  
439 105–110.
- 440 [17] F. Tauro, M. Porfiri, S. Grimaldi, Orienting the camera and firing lasers  
441 to enhance large scale particle image velocimetry for streamflow moni-  
442 toring, Water Resources Research 50 (9) (2014) 7470–7483.
- 443 [18] F. Tauro, S. Grimaldi, A. Petroselli, M. Porfiri, Fluorescent particle

- 444 tracers in surface hydrology: a proof of concept in a natural stream,  
445 Water Resources Research 48 (6) (2012) W06528.
- 446 [19] F. Tauro, S. Grimaldi, A. Petroselli, M. C. Rulli, M. Porfiri, Fluorescent  
447 particle tracers in surface hydrology: a proof of concept in a semi-natural  
448 hillslope, Hydrology and Earth System Sciences 16 (8) (2012) 2973–2983.
- 449 [20] E. Palermo, Drones could grow to \$11 billion industry by 2024, live-  
450 science.com.
- 451 [21] T. Clarke, Pilotless research aircraft: Flying free, Nature 417 (2002)  
452 582–583.
- 453 [22] J. Cohen, Drone spy plane helps fight California fires, Science 318 (5851)  
454 (2007) 727.
- 455 [23] A. Eltner, P. Baumgart, H.-G. Maas, D. Faust, Multi-temporal UAV  
456 data for automatic measurement of rill and interrill erosion on loess soil,  
457 Earth Surface Processes and Landforms 40 (6) (2015) 741–755.
- 458 [24] A. Pérez-Alberti, A. S. Trenhaile, An initial evaluation of drone-based  
459 monitoring of boulder beaches in Galicia, north-western Spain, Earth  
460 Surface Processes and Landforms 40 (1) (2014) 105–111.
- 461 [25] A. J. S. McGonigle, A. Aiuppa, G. Giudice, G. Tamburello, A. J. Hod-  
462 son, S. Guerrieri, Unmanned aerial vehicle measurements of volcanic car-  
463 bon dioxide fluxes, Geophysical Research Letters 35 (6) (2008) L06303.
- 464 [26] L. Shelley, L. Knuth, J. J. Cassano, Estimating sensible and latent heat  
465 fluxes using the integral method from in situ aircraft measurements,

- 466 Journal of Atmospheric and Oceanic Technology 31 (9) (2014) 1964–  
467 1981.
- 468 [27] R. Schiffman, Drones flying high as new tool for field biologists, *Science*  
469 344 (6183) (2014) 459.
- 470 [28] J. Jensen, Biophysical remote sensing, *Annals of the Association of*  
471 *American Geographers* 73 (1) (1983) 111–132.
- 472 [29] J. S. Famiglietti, A. Cazenave, A. Eicker, J. T. Reager, M. Rodell,  
473 I. Velicogna, Satellites provide the big picture, *Science* 349 (6249) (2015)  
474 684–685.
- 475 [30] W. W. Immerzeel, P. D. A. Kraaijenbrink, J. M. Shea, A. B. Shrestha,  
476 F. Pellicciotti, M. F. P. Bierkens, S. M. deJong, High-resolution mon-  
477 itoring of Himalayan glacier dynamics using unmanned aerial vehicles,  
478 *Remote Sensing of Environment* 150 (2014) 93–103.
- 479 [31] <http://www.dji.com/> (2014).
- 480 [32] M. Raffel, C. E. Willert, S. T. Wereley, J. Kompenhans, *Particle Image*  
481 *Velocimetry. A practical guide.*, Springer, New York, 2007.
- 482 [33] I. Fujita, T. Hino, Unseeded and seeded PIV measurements of river flows  
483 video from a helicopter, *Journal of Visualization* 6 (3) (2003) 245–252.
- 484 [34] I. Fujita, Y. Kunita, Application of aerial LSPIV to the 2002 flood of  
485 the Yodo River using a helicopter mounted high density video camera,  
486 *Journal of Hydro-Environment Research* 5 (4) (2011) 323 – 331.

- 487 [35] <http://www.wmo.int> (2015).
- 488 [36] J. L. Coolidge, A historically interesting formula for the area of a quadri-  
489 lateral, *American Mathematical Monthly* 46 (1939) 345–347.
- 490 [37] R. S. Hunter, Photoelectric color difference meter, *Journal of the Optical*  
491 *Society of America* 48 (12) (1958) 985–993.
- 492 [38] F. Tauro, M. Porfiri, S. Grimaldi, Fluorescent eco-particles for surface  
493 flow physics analysis, *AIP Advances* 3 (3) (2013) 032108.
- 494 [39] F. Tauro, E. Rapiti, J. F. Al-Sharab, L. Ubertini, S. Grimaldi, M. Porfiri,  
495 Characterization of eco-friendly fluorescent nanoparticle doped-tracers  
496 for environmental sensing, *Journal of Nanoparticle Research* 15 (9)  
497 (2013) 1884.
- 498 [40] L. Gui, EDPIV - Evaluation Software for Digital Particle Image Ve-  
499 locimetry, <http://lcgui.net> (2013).
- 500 [41] M. Detert, V. Weitbrecht, A vehicle airborne velocimetry system: proof  
501 of concept, *Journal of Hydraulic Research* 53 (4) (2015) 532.
- 502 [42] F. Tauro, C. Pagano, P. Phamduy, S. Grimaldi, M. Porfiri, Large-  
503 scale particle image velocimetry from an unmanned aerial vehicle,  
504 *IEEE/ASME Transactions on Mechatronics* 20 (6) (2015) 3269–3275.
- 505 [43] F. Tauro, A. Petroselli, E. Arcangeletti, Assessment of drone-based sur-  
506 face flow observations, *Hydrological Processes* 30 (7) (2015) 1114–1130.
- 507 [44] F. Tauro, S. Grimaldi, M. Porfiri, Unraveling flow patterns through  
508 nonlinear manifold learning, *PLoS ONE* 9 (3) (2014) e91131.

- 509 [45] F. Tauro, A. Petroselli, M. Porfiri, L. Giandomenico, G. Bernardi,  
510 F. Mele, D. Spina, S. Grimaldi, A novel permanent gauge-cam station  
511 for surface flow observations on the Tiber river, *Geoscientific Instrumentation, Methods and Data Systems* Under review.
- 513 [46] F. Tauro, G. Olivieri, A. Petroselli, M. Porfiri, S. Grimaldi, Flow monitoring with a camera: a case study on a flood event in the Tiber River,  
514 *Environmental Monitoring and Assessment* 188 (2) (2015) 118.
- 516 [47] C.-L. Chiu, Entropy and probability concepts in hydraulics, *Journal of Hydraulic Engineering* 113 (5) (1987) 583–599.
- 518 [48] C.-L. Chiu, Entropy and 2-D velocity distribution in open channels,  
519 *Journal of Hydraulic Engineering* 114 (7) (1988) 738–756.
- 520 [49] G. Farina, S. Alvisi, M. Franchini, T. Moramarco, Three methods for  
521 estimating the entropy parameter M based on a decreasing number of  
522 velocity measurements in a river cross-section, *Entropy* 16 (5) (2014)  
523 2512–2529.
- 524 [50] C.-L. Chiu, Application of entropy concept in open channel flow study,  
525 *Journal of Hydraulic Engineering* 117 (5) (1991) 615–628.
- 526 [51] R. Xia, Relation between mean and maximum velocities in a natural  
527 river, *Journal of Hydraulic Engineering* 123 (8) (1997) 720–723.



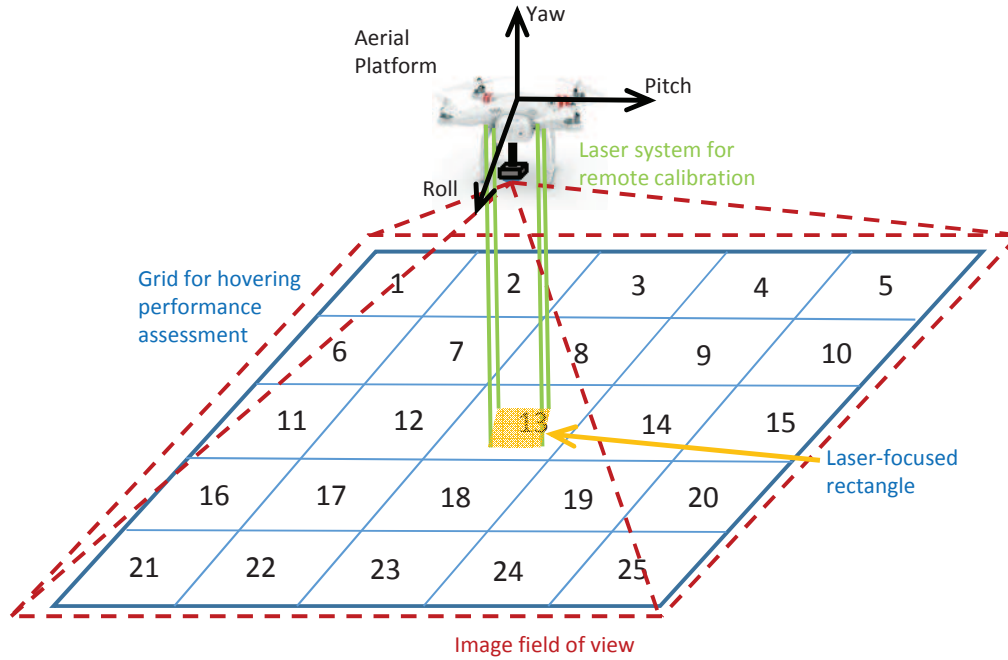


Figure 1: Sketch of the experimental setup. Analysis of the squares of the grid was used to assess the ability to capture stable videos.

Table 1: Velocity measurements performed on the natural stream. Symbols  $v_m$  and  $\sigma$  stand for average maximum velocity and standard deviation, respectively. Average maximum velocities and standard deviations from the drone are obtained from LSPIV time-averaged maps by averaging over the yellow dashed subarea reported in Figure 3.

	$v_m$ [m/s]	$\sigma$ [m/s]
Flowmeter	2.54	0.09
Drone		
artificial tracers	2.29	0.09
natural tracers	2.15	0.27

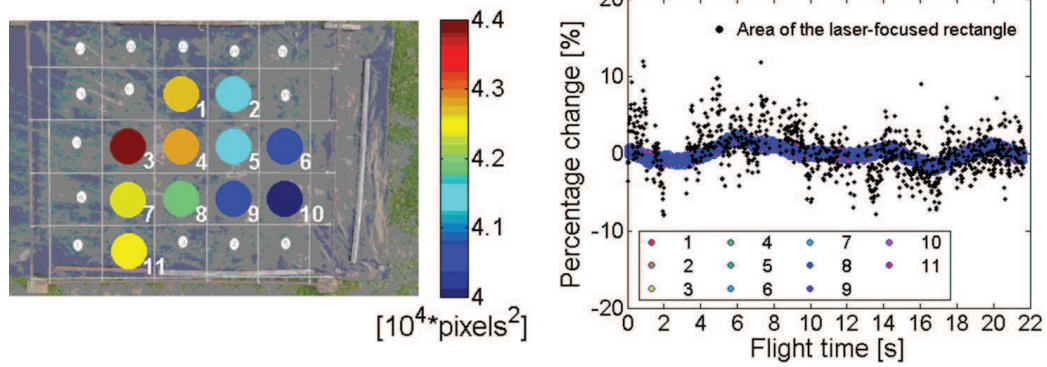


Figure 2: Left, experimental grid for assessing the drone's hovering capability. Colored markers inside each square indicate the average area in pixels. Right, time histories of the area of each of the 11 squares visible during the flight (colored dots), and of the area of the rectangle focused by the laser beams (black dots). Raw data are smoothed through a local regression filter with weighted linear least squares and a parabolic model.

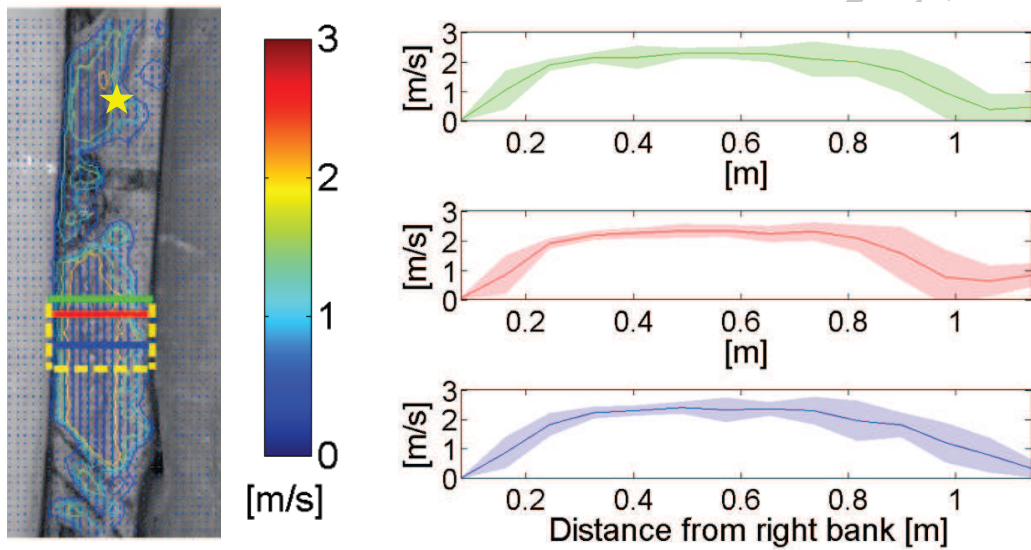


Figure 3: Left, representative surface flow velocity maps from the aerial platform based on the use of natural floaters. The yellow star indicates the location at which measurements with the impeller flowmeter are taken. Right, time-averaged cross-sectional profiles corresponding to the green, red, and blue cross-sections highlighted in the map. Shaded areas indicate standard deviations. The yellow dashed box in the left panel highlights the subarea used for measurement comparison.

- The integration of optical techniques and drones can help in flow monitoring
- Sub-meter channel flow is noninvasively monitored from a low-cost drone
- Surface flow measurements from the drone are in agreement with traditional methods
- Quality of images captured from the drone yields accurate flow measurements

ACCEPTED MANUSCRIPT